Supporting Information

A wide bandgap polymer donor composed of benzodithiophene and oxime substituted thiophene for high-performance organic solar cells

*Keqiang He, Pankaj Kumar, Yi Yuan, Zhifang Zhang, Xu Li, Haitao Liu, Jinliang Wang, Yuning Li**

Dr. K. He, P. Kumar, Z. Zhang, Dr. X. Li, H. Liu, Prof. Dr. Y. Li, Department of Chemical Engineering and Waterloo Institute of Nanotechnology (WIN), University of Waterloo, 200 University Ave West, N2L 3G1, Canada. E-mail: Yuning.li@uwaterloo.ca

Dr. X. Li, H. Liu, J. Wang, Institute of Chemistry, Henan Academy of Sciences, 56 Hongzhuan Road, Jinshui District, Zhengzhou, Henan, China, 450002A

Corresponding Author

Prof. Dr. Y. Li, Department of Chemical Engineering and Waterloo Institute of Nanotechnology (WIN), University of Waterloo, 200 University Ave West, N2L 3G1, Canada. E-mail: yuning.li@uwaterloo.ca

Synthesis of 2,5-dibromothiophene-3-carbaldehyde (2)

This compound was synthesized according to literature method.[1,2]

A solution of N-bromosuccinimide (NBS) (35.7 g, 200 mmol) in DMF (100 mL) was added dropwise into a solution of 3-thiophenecarboxaldehyde (**1**) (9 g, 80 mmol) in DMF (120 mL) in a 250 mL round bottom flask. Then the reaction mixture was stirred for 24 h at room temperature in the dark. The mixture was poured into water and extracted with diethyl ether. The organic phase was washed with brine and dried over anhydrous Na_2SO_4 and then solvent was removed by rotary evaporation. The crude product was purified by column chromatography on silica gel using a mixture of hexane and dichloromethane (v/v = 3/1) as the eluent to obtain **2** as a white solid. Yield: 16.2 g (75%). ^{1}H NMR (300 MHz, $CDCl_3$, ppm) δ: 9.80 (s, 1H), 7.34 (s, 1H).

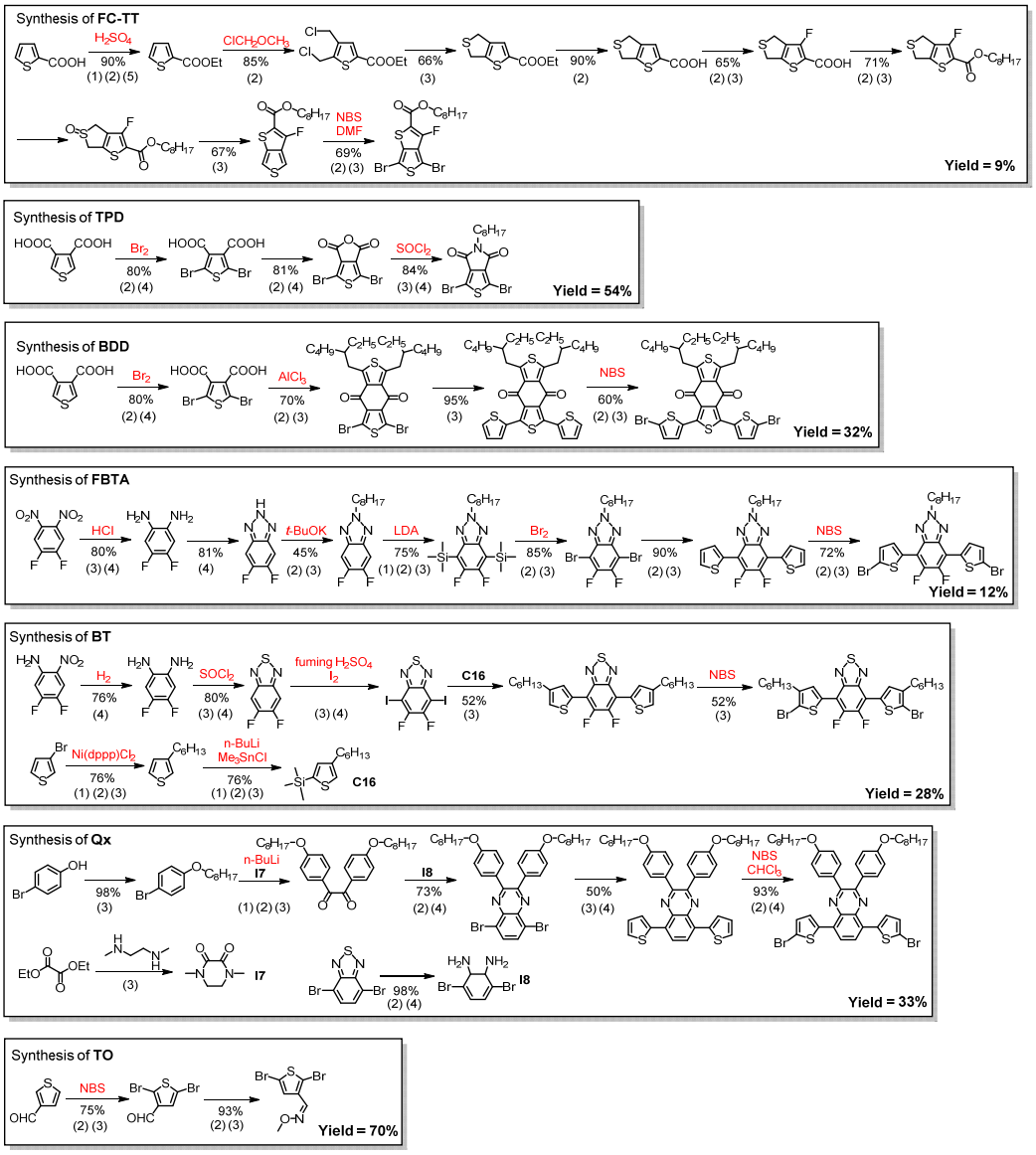

Figure S1. Synthetic routes and overall yield for most widely reported acceptor units used in BDT based polymer donors and TO unit. The red fonts represent the hazardous or dangerous chemicals used in the synthesis. The codes of the unit operations are: (1) Quenching/neutralization; (2) Extraction; (3) Column chromatography; (4) Recrystallization; (5) Distillation/sublimation.[3]

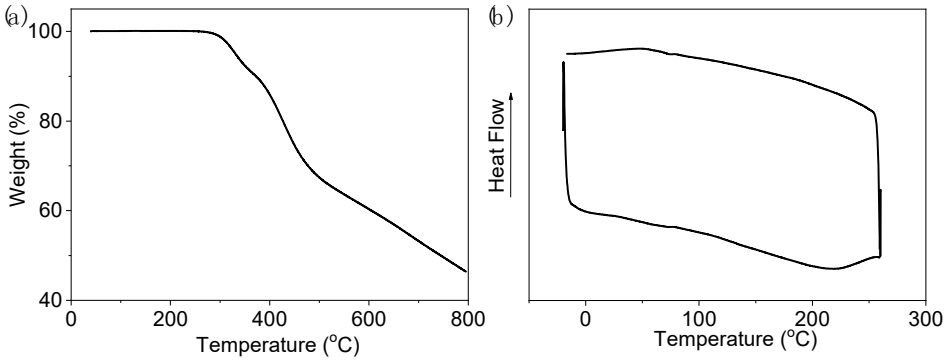

Figure S2. TGA (a) and DSC (b) curves of PBDTTO.

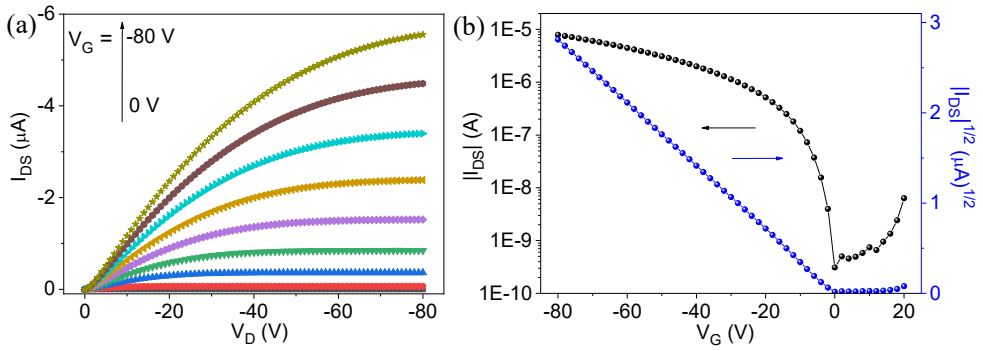

Figure S3. Typical output (a) and transfer (V_{DS} = -80 V) (b) curves of OTFT devices based on PBDTTO.

Table S1. OTFT device performances of PBDTTO.

Process (°C)	μ_{avg} ± std ($cm^2V^{-1}s^{-1}$)	μ_{max} ($cm^2V^{-1}s^{-1}$)	V_T (V)	$I_{on/off}$
rt	5.36E-3 ± 2.42E-4	5.66E-3	-5 - 1	10^4
50	5.98E-3 ± 1.70E-4	6.19E-3	-7 - -3	10^4
100	5.56E-3 ± 1.08E-4	5.72E-3	-2 - 2	10^4
150	6.23E-3 ± 9.67E-5	6.33E-3	-2 - 2	10^4
200	4.74E-3 ± 5.70E-5	4.80E-3	-8 - -6	10^5

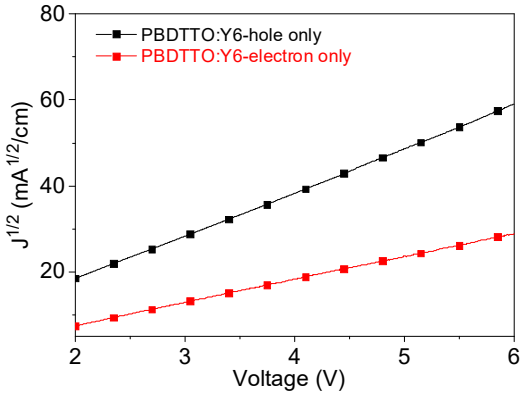

Figure S4. $J^{1/2}$-V curves of hole-only and electron-only devices of PBDTTO:Y6 by fitting the modified Mott-Gurney equation: $J = 9\mu\varepsilon\varepsilon_0 V^2/8L^3$.

Table S2. SCLC mobilities of PBDTTO neat film and PBDTTO:Y6 blend films annealed at 130 °C.

	PBDTTO, μ_{max} (μ_{avg} ± std)	PBDTTO:Y6, μ_{max} (μ_{avg} ± std)
μ_{hole} ($cm^2V^{-1}s^{-1}$)	2.05E-4 (1.39E-4 ± 5.82E-5)	2.43E-4 (1.73E-4 ± 5.93E-5)
$\mu_{electron}$ ($cm^2V^{-1}s^{-1}$)	--	1.84E-4 (1.40E-4 ± 6.11E-5)

Table S3. Optimization of device performances with different PBDTTO:Y6 (D/A) ratio, annealing temperature, film thickness, solvent additive and annealing solvent.

Condition	J_{SC} (mA/cm^2)	V_{OC} (V)	FF	PCE (%)
Annealing temperature: 100 ºC, Thickness: 100 nm				
1:1	24.61 (25.12 ± 0.63)	0.85 (0.84 ± 0.01)	0.54 (0.52 ± 0.01)	11.30 (11.05 ± 0.18)
1.2:1	20.94 (20.57 ± 0.32)	0.87 (0.87 ± 0.00)	0.52 (0.52 ± 0.00)	9.44 (9.31 ± 0.10)
1:1.2	23.52 (23.67 ± 0.29)	0.90 (0.88 ± 0.02)	0.55 (0.54 ± 0.02)	11.64 (11.30 ± 0.47)
D/A Ratio: 1:1.2, Thickness: 100 nm,				
RT	23.53 (21.80 ± 1.13)	0.89 (0.90 ± 0.01)	0.54 (0.56 ± 0.01)	11.23 (10.97 ± 0.27)
100 ºC	23.52 (23.67 ± 0.29)	0.90 (0.88 ± 0.02)	0.55 (0.54 ± 0.02)	11.64 (11.30 ± 0.47)
130 ºC	27.03 (26.48 ± 1.00)	0.83 (0.82 ± 0.01)	0.59 (0.60 ± 0.02)	13.29 (12.99 ± 0.34)
160 ºC	23.95 (23.28 ± 1.69)	0.80 (0.82 ± 0.05)	0.61 (0.59 ± 0.05)	11.84 (11.22 ± 0.55)
D/A Ratio: 1:1.2, Annealing temperature: 130 ºC				
120 nm	24.42 (23.65 ± 0.57)	0.82 (0.81 ± 0.01)	0.54 (0.55 ± 0.01)	10.88 (10.55 ± 0.30)
100 nm	27.03 (26.48 ± 1.00)	0.83 (0.82 ± 0.01)	0.59 (0.60 ± 0.02)	13.29 (12.99 ± 0.34)
80 nm	25.37 (24.69 ± 1.34)	0.87 (0.86 ± 0.00)	0.57 (0.57 ± 0.01)	12.59 (12.11 ± 0.59)
D/A Ratio: 1:1.2, Annealing temperature: 130 ºC, Thickness: 100 nm				
None	27.03 (26.48 ± 1.00)	0.83 (0.82 ± 0.01)	0.59 (0.60 ± 0.02)	13.29 (12.99 ± 0.34)
DIO-0.5% v/v	24.62 (24.25 ± 1.03)	0.74 (0.75 ± 0.01)	0.66 (0.66 ± 0.01)	12.02 (11.96 ± 0.08)
D/A Ratio: 1:1.2, Annealing temperature: 130 ºC, Thickness: 100 nm				
None	27.03 (26.48 ± 1.00)	0.83 (0.82 ± 0.01)	0.59 (0.60 ± 0.02)	13.29 (12.99 ± 0.34)
CF anneal	27.42 (26.86 ± 0.84)	0.82 (0.82 ± 0.00)	0.59 (0.58 ± 0.02)	13.22 (12.77 ± 0.32)
THF anneal	27.47 (26.66 ± 0.57)	0.83 (0.82 ± 0.00)	0.57 (0.57 ± 0.01)	13.03 (12.52 ± 0.36)

Table S4. Photovoltaic parameters of the OSCs based on PTOBDT:ITIC (1:1).[a]

Temperature	J_{SC} (mA/cm^2)	V_{OC} (V)	FF	PCE (%)
RT	18.02	0.95	0.64	10.99
100 °C	17.57	0.96	0.69	11.64
130 °C	17.41	0.88	0.48	7.40

[a] Devioces were fabricated and characterized using the similar methods for the OSCs basd on PBDTTO:Y6.

Table S5. Performances of a PBDTTO:Y6 based OSC device after storage for different periods of time under ambient conditions without encapsulation.

Time (d)	J_{SC} (mA/cm^2)	V_{OC} (V)	FF	PCE (%)	PEC retention (%)	R_S (ohmcm^2)	R_{sh} (ohm cm^2)
0	27.03	0.83	0.59	13.29		2	447.79
9	26.76	0.81	0.52	11.33	85	4.97	320.87
15	26.21	0.8	0.47	9.73	73	5.59	291.67
30	25.48	0.79	0.45	8.95	67	9.59	127.34

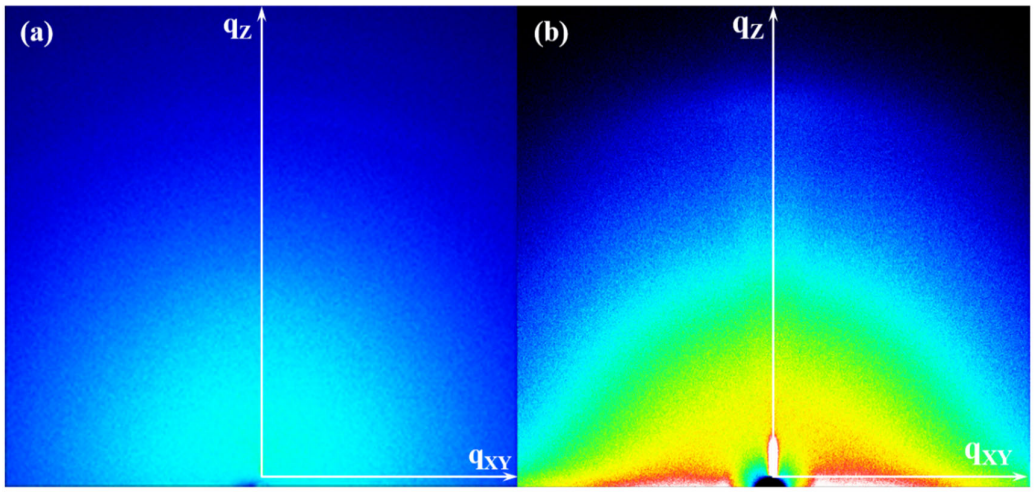

Figure S5. 2D-GIXD patterns of the PBDTTO film (a) and PBDTTO:Y6 blend film (b).

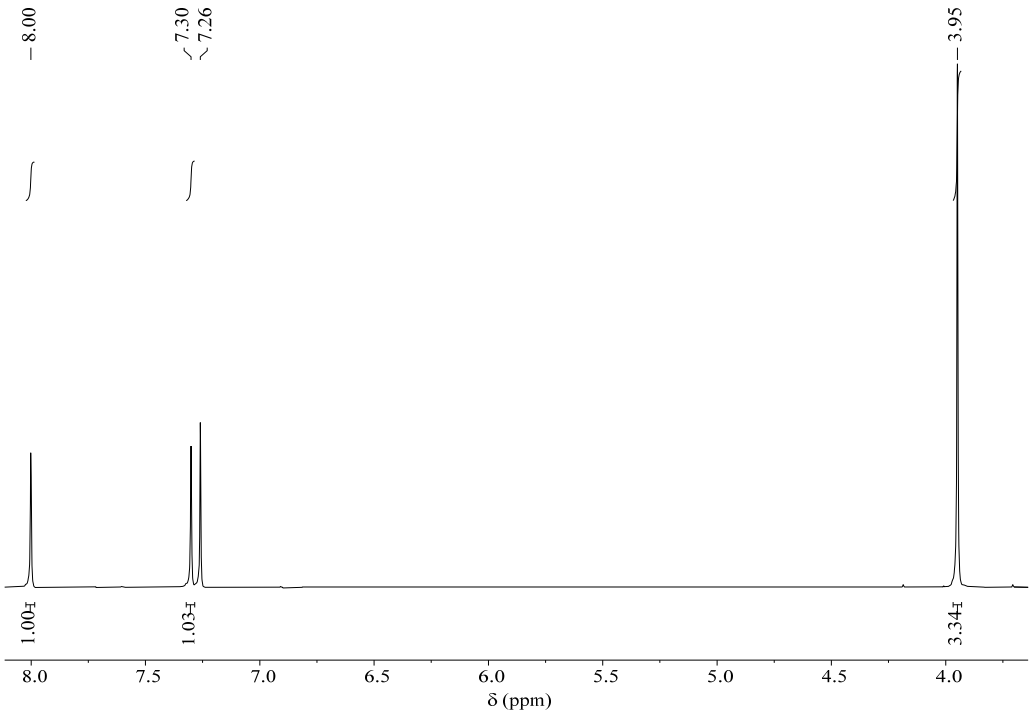

Figure S6. ^{1}H NMR spectra of compound **3**.

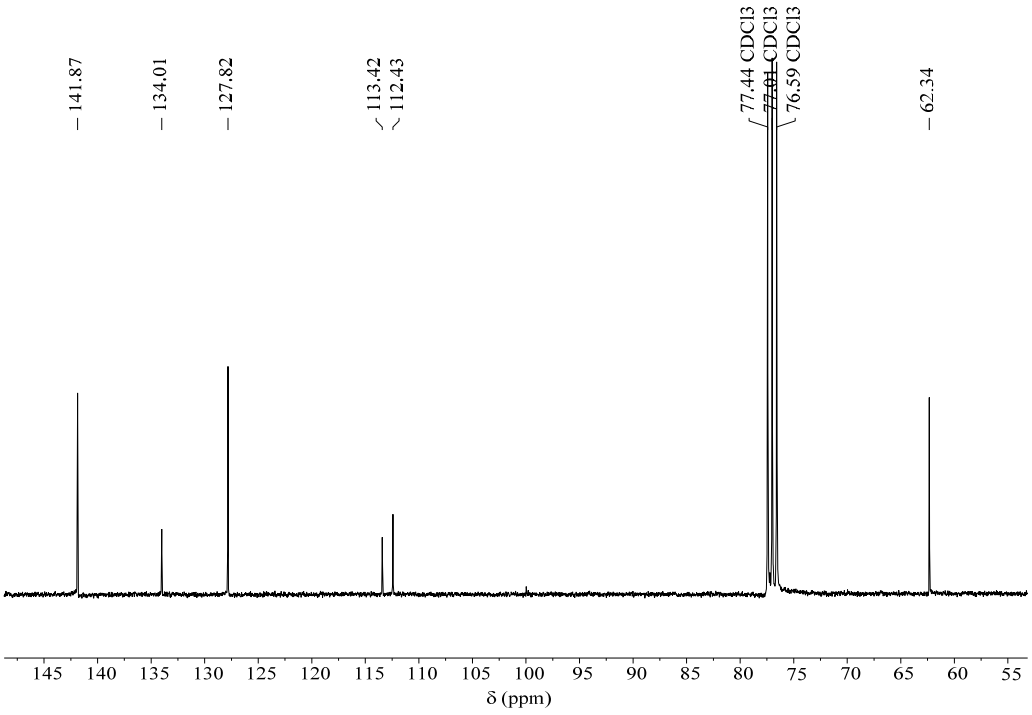

Figure S7. ^{13}C NMR spectra of compound **3**.

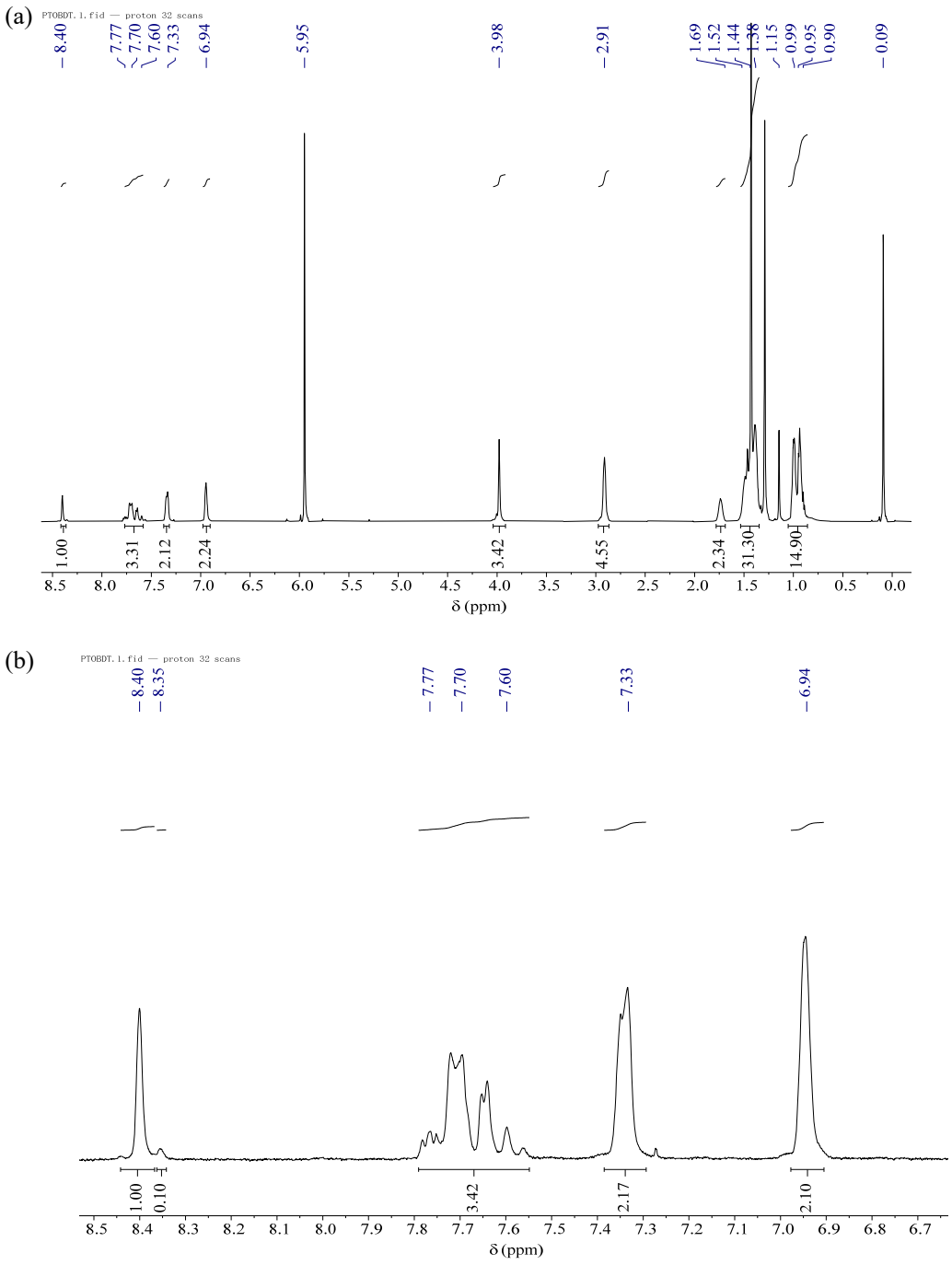

Figure S8. ^{1}H NMR spectra of PBDTTO: (a) full scale and (b) zoomed aromatic region.

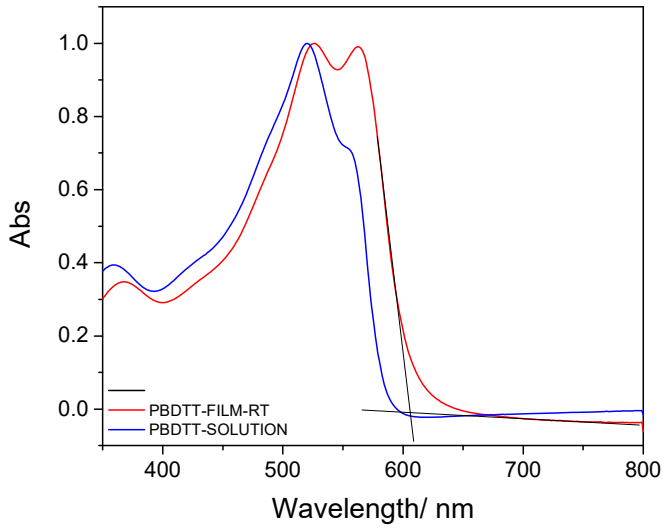

Figure S9. UV-vis spectra of PBDT-Th measure in solution (chlorobenzene) and in an as-cast film. The optical band gap of PBDT-Th is calculated to be 2.05 eV.

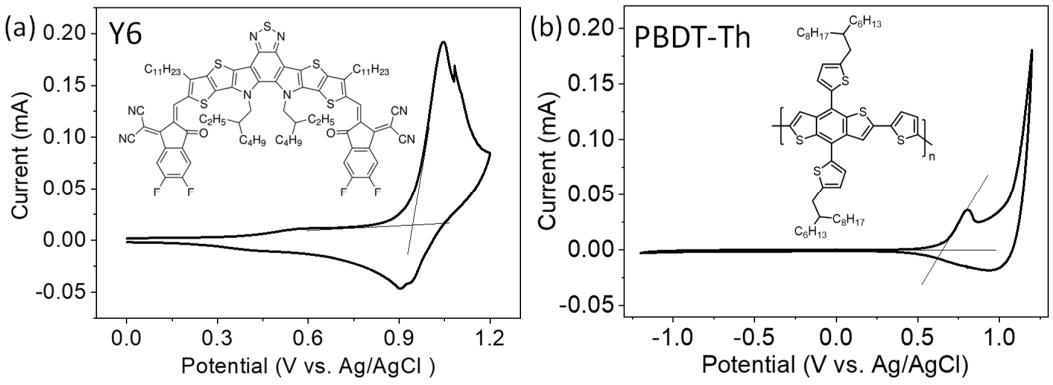

Figure S10. cyclic voltammograms of (a) Y6 and (b) PBDT-Th using Ag/AgCl as a reference electrode using 0.1 M *n*-Bu_4NPF_6 in dry acetonitrile as an electrolyte under nitrogen at a scan rate of 100 mVs^{-1}. The E_{HOMO} values are calculated to be -5.74 eV for Y6 and -5.45 eV for PBDT-Th using their onset potentials of 0.94 V and 0.65 V, respectively, using reference as a reference (E_{HOMO} = -4.80 eV).

References

(1) Luo, X.; Wu, F.; Xiao, H.; Guo, H.; Liu, Y.; Tan, S. Synthesis and Photovoltaic Properties of the Copolymers Containing Zinc Porphyrin Derivatives as Pendant Groups. *Synthetic Metals* **2017**, *223*, 205–211. https://doi.org/10.1016/j.synthmet.2016.11.026.

(2) Chen, D.; Yao, J.; Chen, L.; Yin, J.; Lv, R.; Huang, B.; Liu, S.; Zhang, Z.-G.; Yang, C.; Chen, Y.; Li, Y. Dye-Incorporated Polynaphthalenediimide Acceptor for Additive-Free High-Performance All-Polymer Solar Cells. *Angew. Chem. Int. Ed.* **2018**, *57* (17), 4580–4584. https://doi.org/10.1002/anie.201800035.

(3) Po, R.; Bianchi, G.; Carbonera, C.; Pellegrino, A. "All That Glisters Is Not Gold": An Analysis of the Synthetic Complexity of Efficient Polymer Donors for Polymer Solar Cells. *Macromolecules* **2015**, *48* (3), 453–461. https://doi.org/10.1021/ma501894w.